

# Relative roles of surface temperature and climate forcing patterns in the inconstancy of radiative feedbacks

A. D. Haugstad<sup>1</sup>, K. C. Armour<sup>1,2</sup>, D. S. Battisti<sup>1</sup> and B. E. J. Rose<sup>3</sup>

<sup>1</sup> Department of Atmospheric Sciences, University of Washington, Seattle, WA 98195

<sup>2</sup> School of Oceanography, University of Washington, Seattle, WA 98195

<sup>3</sup> Department of Atmospheric and Environmental Sciences, University at Albany, State University of New York, Albany, NY 12222

Corresponding author: Alexander Haugstad (ahaugsta@uw.edu)

## Key Points:

- Radiative feedbacks predominantly depend on the spatial pattern of surface temperature change, regardless of how that pattern is forced
- Climate model experiments using prescribed sea-surface temperature patterns are useful to study radiative feedbacks and climate sensitivity
- Uniform warming simulations such as the amip4K runs produce different feedbacks than under polar amplified warming

This article has been accepted for publication and undergone full peer review but has not been through the copyediting, typesetting, pagination and proofreading process which may lead to differences between this version and the Version of Record. Please cite this article as doi: 10.1002/2017GL074372

## Abstract

Radiative feedbacks robustly vary over time in transient warming simulations. Published studies offer two explanations: (i) evolving patterns of ocean heat uptake (OHU) or radiative forcing give rise to OHU or forcing ‘efficacies’, and (ii) evolving patterns of surface temperature change. This study seeks to determine whether these explanations are indeed distinct. Using an idealized framework of an aquaplanet atmosphere-only model, we show radiative feedbacks depend on the pattern of climate forcing. Yet, the same feedbacks arise when the temperature pattern induced by that climate forcing is prescribed in the absence of any forcing. These findings suggest the perspective that feedbacks are influenced by ‘efficacies’ of forcing and OHU is equivalent to the perspective that feedbacks are dependent on the temperature patterns induced by those forcings. These findings suggest that prescribed surface temperature simulations are valuable for studying the temporal evolution of radiative feedbacks.

## 1 Introduction

Radiative feedbacks describe the response of top-of-atmosphere (TOA) radiation to a change in surface temperature, as commonly expressed by the standard model of global TOA energy balance,

$$\bar{Q} = \lambda \bar{T} + \bar{R} , \quad (1)$$

where the overbar denotes an area-weighted global mean quantity,  $\bar{R}$  is the radiative forcing,  $\bar{Q}$  the TOA radiative imbalance,  $\lambda$  the global radiative feedback, and  $\bar{T}$  the surface temperature response.  $\bar{Q}$  and  $\bar{R}$  are positive downward; a negative value for  $\lambda$  represents a stabilizing feedback, with a more negative value corresponding to a less sensitive climate.

Feedbacks are often considered to be time-invariant, meaning that the value of  $\lambda$  at any given time is assumed to be equal to the radiative feedback at equilibrium ( $\equiv \lambda_{eq}$ ). However, studies have found that  $\lambda$  changes over time in transient simulations of global climate models (GCMs)—and generally in the direction that climate becomes more sensitive to greenhouse gas forcing as equilibrium is approached ( $\lambda < \lambda_{eq}$ ) [Murphy, 1995; Senior and Mitchell, 2000; Gregory *et al.*, 2004; Williams *et al.*, 2008; Winton *et al.*, 2010; Armour *et al.*, 2013; Frölicher *et al.*, 2013; Rose *et al.*, 2014; Andrews *et al.*, 2015; Knutti and Rugenstein, 2015; Gregory, 2015; Marvel *et al.*, 2015; Paynter *et al.*, 2015; Gregory and Andrews, 2016; Rugenstein *et al.*, 2016; Rose and Rayborn, 2016; Armour, 2017]. This time variation of  $\lambda$  implies that long-term global warming may be substantially underestimated by projections that assume constant feedbacks, posing a major challenge to future climate prediction and past climate record interpretation [Armour *et al.*, 2013; Marvel *et al.*, 2015; Forster, 2016; Armour, 2016; Armour, 2017].

What processes cause feedbacks to change under transient warming? One proposed mechanism is that  $\lambda$  depends on the spatial pattern of forcing acting on the atmosphere – either radiatively at the TOA or as ocean heat uptake (OHU) at the sea surface; feedbacks thus vary as the forcing pattern changes over time [Winton *et al.*, 2010; Rose *et al.*, 2014; Kang and Xie, 2014; Marvel *et al.*, 2015; Rugenstein *et al.*, 2016; Trossman *et al.*, 2016]. For example, under transient warming, OHU preferentially occurs within the Southern Ocean and North Atlantic Ocean due to regional ocean circulations [Marshall *et al.*, 2015; Armour *et al.*, 2016]; this OHU pattern is distinct from the pattern of CO<sub>2</sub> forcing, which peaks in the tropics, giving rise to a different value of  $\lambda$  under transient warming relative to the equilibrium response to CO<sub>2</sub> forcing [e.g., Winton *et al.*, 2010; Rose *et al.*, 2014; Rugenstein *et al.*, 2016]. Different radiative forcing agents, such as tropospheric aerosols, also have

patterns of forcing that are distinct from that of CO<sub>2</sub> [e.g., *Hansen et al.*, 2005] and thus different values of  $\lambda$  [*Shindell*, 2014; *Marvel et al.*, 2015]. These forcing pattern effects are commonly characterized in terms of a so-called forcing “efficacy”, defined as the ratio of global-mean surface warming that occurs in response to a given forcing relative to that under a CO<sub>2</sub> forcing of the same magnitude [*Hansen et al.*, 2005; *Winton et al.*, 2010].

Equivalently, the efficacies of radiative forcing and OHU are equal to the ratio of the value of  $\lambda$  they induce to the value of  $\lambda_{\text{eq}}$  induced by CO<sub>2</sub> forcing alone [*Rose et al.*, 2014; *Rose and Rayborn*, 2016]. This principle has been cleanly demonstrated within atmospheric GCM simulations where OHU patterns are induced via prescribed sea-surface heat fluxes: distinct heat flux patterns with identical global mean values drive different global surface temperature responses [*Rose et al.*, 2014; *Kang and Xie*, 2014; *Rugenstein et al.*, 2016].

The inconstancy of  $\lambda$  could also be due to the global radiative response to warming depending not just on  $\bar{T}$ , but also on the pattern of sea surface temperature change, which evolves in time during transient warming [*Armour et al.*, 2013; *Andrews et al.*, 2015; *Gregory and Andrews*, 2016; *Zhou et al.*, 2016]. For example, the Southern Ocean is slow to warm in greenhouse gas forcing simulations, but eventually warms substantially [*Armour et al.*, 2016]; consequently,  $\lambda$  changes over time as Southern Ocean feedbacks slowly become activated [*Armour et al.*, 2013]. Moreover, changes in the zonal temperature gradient within the equatorial Pacific Ocean appear to induce changes in tropical cloud feedbacks by modifying lower tropospheric stability and stratocumulus cloud cover [*Andrews et al.*, 2015; *Gregory and Andrews*, 2016; *Zhou et al.*, 2016]. In this view, distinct values of  $\lambda$  arise from different spatial patterns of warming, regardless of how those warming patterns arise or change over time. The time-variation of  $\lambda$  has been studied within atmospheric GCM simulations driven by prescribed sea-surface temperature (SST) patterns, without consideration of the pattern of OHU [e.g., *Gregory and Andrews*, 2016; *Zhou et al.*, 2016].

Of course, OHU and surface temperature evolve due to a prescribed radiative forcing, precluding determination of the dominant mechanisms governing the inconstancy of feedbacks. It is plausible that radiative feedbacks depend on both the pattern of forcing and surface temperature change simultaneously. In other words, one interpretation of forcing “efficacy” is that distinct feedbacks arise from different patterns of surface temperature changes which, in turn, are induced by different patterns of climate forcing [e.g. *Shindell et al.*, 2014; *Marvel et al.*, 2015; *Rugenstein et al.*, 2016]. It is thus important to quantify to what degree the radiative feedbacks depend on the spatial patterns of SSTs relative to the surface heat fluxes that induce those SST patterns [*Rugenstein et al.*, 2016]. This directly informs our understanding of how feedbacks can be studied within both GCMs and observations: do feedbacks depend on the spatial pattern of forcing, temperature change, or both simultaneously?

In this study, we perform model simulations designed to explicitly compare these explanations and determine (i) to what extent feedbacks depend on the structure and type of forcing applied, (ii) to what extent feedbacks depend on the pattern of surface temperature change induced by that forcing, and (iii) to what extent these mechanisms can be separated from one another. We use an idealized aquaplanet model with suites of prescribed forcings and SST boundary conditions to evaluate how radiative feedbacks behave when the patterns of forcing or surface temperature are changed individually. Our results will inform on the validity of prescribed SST simulations—both past and future—for diagnosing radiative feedbacks.

## 2 Methods

We use the aquaplanet version of AM2.1 (GFDL Global Atmospheric Model Development Team 2004), the atmospheric component of the Geophysical Fluid Dynamics Laboratory (GFDL) Climate Model (CM2.1). AM2.1 is among the small ensemble of models used by *Rose et al.* [2014] in their analysis of varying patterns of OHU. We keep all model specifications the same as in *Rose et al.*; sea-surface albedo is uniformly set to 0.1 with no sea ice (SST is allowed to drop below 0°C) and all simulations are run at perpetual equinox. Grid resolution for this model is  $\sim 2^\circ$  latitude  $\times$   $2.5^\circ$  longitude, with 24 vertical levels.

We perform two types of simulations. The first type uses AM2.1 coupled to a ‘slab ocean’ (with depth fixed at 10 m), in which we prescribe distinct patterns of forcing. These patterns are either TOA radiative changes due to a change in CO<sub>2</sub> or sea-surface heat flux changes induced via heat sinks/sources within the slab ocean layer (representing OHU). All forcings are zonally uniform and the simulations are 100 years long (we analyze only the last 60 years, once steady-state has been achieved). We denote this set of simulations with the prefix “SL\_” before the experiment name. The slab ocean allows for heat exchange between the ocean surface and the atmosphere, but has no heat transport between adjacent ocean grid cells. Thus, any applied heat sink/source within the ocean slab requires the same amount of heat to be exchanged between the ocean surface and the atmosphere in equilibrium; without any heat sinks/sources, net surface heat fluxes are zero everywhere once equilibrium is reached.

The second type of simulations are prescribed SST experiments, in which we prescribe a zonally uniform profile of SST (symmetrized about the equator). We denote these experiments with the prefix “SST\_”. We run these simulations for 40 years each, a length of time required to produce steady results in the presence of unforced variability in TOA radiation, and analyze only the last 35 years to allow for model spin-up. Within these simulations, net surface heat fluxes can be nonzero. The sign convention for surface heat fluxes is positive downward. Table 1 summarizes our various simulations.

## 3 Results

We first consider a simulation with AM2.1 coupled to the slab ocean in which we double CO<sub>2</sub> and allow the system to equilibrate (denoted SL\_2xCO<sub>2</sub>). This produces a pattern of surface temperature change  $T(\varphi)$ , where  $\varphi$  is latitude, relative to a slab ocean control simulation (SL\_CTL). Following *Rose et al.* [2014], we analyze the response in terms of a local energy budget equation:

$$Q(\varphi) = \lambda(\varphi)T(\varphi) + R(\varphi) - \nabla \cdot F(\varphi) \quad , \quad (2)$$

where each term is a zonal mean quantity:  $Q(\varphi)$  is the net sea-surface heat flux;  $R(\varphi)$  is the radiative forcing;  $\lambda(\varphi)$  is the radiative feedback; and  $\nabla \cdot F(\varphi)$  is the meridional heat flux divergence.

We treat the resulting patterns of feedback and warming from CO<sub>2</sub> doubling as a benchmark for comparison to subsequent simulations. The temperature response shows polar amplified warming with a global mean warming of 3.01 K (Fig. 1b). To calculate the radiative feedbacks in the presence of CO<sub>2</sub> changes, we must account for the TOA radiation changes associated with CO<sub>2</sub> radiative forcing. We thus perform a simulation in which climatological SSTs from the slab ocean control simulation (SL\_CTL) are prescribed and held fixed while CO<sub>2</sub> is doubled (denoted SST\_CTLw/2xCO<sub>2</sub>); the net TOA radiation anomaly (relative to SST\_CTL) gives the effective CO<sub>2</sub> radiative forcing  $R(\varphi)$  including tropospheric

adjustments [e.g., *Andrews and Forster, 2008; Hansen et al., 2005*] (Fig. 2a). In an aquaplanet, this adjusted forcing does not include any adjustments that would result from the inclusion of continents, such as warming over land and associated land-sea contrast, or from rapid changes in ocean circulation (*Rugenstein et al., 2016b*). The total TOA radiation anomaly in SL\_2xCO<sub>2</sub> is equal to  $\lambda(\varphi)T(\varphi) + R(\varphi)$ . Thus, subtracting  $R(\varphi)$  leaves the radiative response to surface warming ( $\lambda(\varphi)T(\varphi)$ ) which yields the local feedback  $\lambda(\varphi)$  when divided by  $T(\varphi)$ . The pattern of  $\lambda(\varphi)$  for SL\_2xCO<sub>2</sub> is everywhere negative, with latitudinal variations within a range of  $-4.0 \text{ Wm}^{-2}\text{K}^{-1}$  to  $0 \text{ Wm}^{-2}\text{K}^{-1}$  (Fig. 1c). Importantly, this feedback pattern arises with zero net surface heat flux (Fig. 1a).

We next perform a simulation wherein the SST warming pattern from SL\_2xCO<sub>2</sub> is prescribed with CO<sub>2</sub> held fixed at its control value (denoted SST\_2xCO<sub>2</sub>). While the patterns of SST are identical in SL\_2xCO<sub>2</sub> and SST\_2xCO<sub>2</sub> by construction (Fig. 1b), the surface heat fluxes are quite different: the surface heat flux under prescribed SSTs is not constrained to be zero as in the slab ocean configuration, and ranges from 2 to 7 W/m<sup>2</sup> out of the ocean (Fig. 1a). Yet, the resulting feedback pattern from SST\_2xCO<sub>2</sub> is nearly identical to that obtained from SL\_2xCO<sub>2</sub> (Fig. 1c). That is, the same feedbacks—both globally and locally—can arise even with distinct patterns of surface heat fluxes, provided that the warming pattern is the same in both cases.

Why does  $\lambda(\varphi)$  appear to be insensitive to the pattern of surface heat fluxes? One might expect that changing latent heat fluxes may affect the atmospheric structure and TOA radiation, e.g., through an effect on low cloud cover. Indeed, a similar set of experiments using large-eddy simulations suggests that the marine boundary layer cloud response to a given warming may be different depending on whether identical SST anomalies are generated interactively by CO<sub>2</sub> forcing or prescribed [*Tan et al., 2017*]. It is not clear why our findings differ from these. It seems possible our coarse resolution atmospheric GCM is not capturing the relevant physical controls on boundary layer clouds. The sensitivity to the lower boundary condition may also arise from the large-eddy simulation setup, with fixed lateral boundary conditions driving a small domain.

However, the results in Fig. 1 make sense in the context of the forcing-feedback framework [*Andrews and Forster, 2008*]—provided we account for tropospheric adjustments to CO<sub>2</sub> forcing in both the TOA radiation fields and sea-surface heat fluxes [*Hansen et al., 2005*]. Summing the response of SST\_CTLw/2xCO<sub>2</sub> with SST\_2xCO<sub>2</sub> results in similar patterns of TOA radiation and sea-surface fluxes to when CO<sub>2</sub> is doubled from its control value while the 2xCO<sub>2</sub> warming pattern is prescribed at the same time (SST\_2xCO<sub>2</sub>w/2xCO<sub>2</sub>; Figs. S1a,b). That is, the response to CO<sub>2</sub> forcing and surface warming is, to a good approximation, equal to the sum of the response to each individually (SST\_2xCO<sub>2</sub>w/2xCO<sub>2</sub> = SST\_CTLw/2xCO<sub>2</sub> + SST\_2xCO<sub>2</sub>). Moreover, the patterns of radiative feedbacks seen under SST\_2xCO<sub>2</sub>w/2xCO<sub>2</sub> and SL\_2xCO<sub>2</sub> are nearly identical (Fig. S1c), consistent with the interpretation that feedbacks depend on the pattern of surface warming, regardless of the forcing that has given rise to that warming pattern.

While the surface heat fluxes in SST\_2xCO<sub>2</sub>w/2xCO<sub>2</sub> approximately average to zero outside of the tropics, they are robustly positive between 30°N and 30°S (Fig. S1b). In contrast, the sea-surface heat fluxes within SL\_2xCO<sub>2</sub> are zero everywhere, as they must be in equilibrium. This discrepancy is likely due to differences arising from whether SST anomalies are prescribed or generated interactively; small differences in the location of the Inter-Tropical Convergence Zone (ITCZ) between these simulations seem to drive substantial changes in the amount of shortwave radiation reaching the surface. However, these

differences appear to have negligible effect on TOA radiation or other model fields. Our interpretation, then, is that the patterns of sea-surface fluxes depend on *both* the applied forcing and the surface temperature response to that forcing; however, when tropospheric adjustments to forcing are properly accounted for, the radiative response (i.e.,  $\lambda(\varphi)$ ) depends only on the pattern of surface warming. This interpretation is expected to hold provided the model response to forcing and surface warming add linearly to the response to both together; it may break down under substantially larger or very localized forcing, and should be tested within more realistic model setups.

Why, then, have feedbacks been found to be sensitive to the pattern of radiative forcing and OHU [e.g. *Rose et al.*, 2014; *Marvel et al.*, 2015; *Rugenstein et al.*, 2016]? To explore this, we use the above methodology with a new set of forcings. We first take the net surface heat fluxes from SST\_2xCO<sub>2</sub> (Figs. 1a and 2a) and prescribe that pattern as OHU in a slab ocean simulation (denoted SL\_QSfc). In another simulation (denoted SL\_QTOA), we apply the TOA radiative forcing associated with CO<sub>2</sub> doubling (Fig. 2a) as OHU in the slab ocean, thus driving the system with the CO<sub>2</sub> forcing pattern at the surface instead of the TOA. These simulations, along with SL\_2xCO<sub>2</sub> and SST\_2xCO<sub>2</sub>, allow us to assess the sensitivity of feedbacks to both the vertical and horizontal structures of forcing, and will collectively be referred to as ‘2xCO<sub>2</sub> Variants’.

Interestingly, the SST responses for SL\_2xCO<sub>2</sub>, SL\_QSfc and SL\_QTOA are nearly identical (Fig. 2b). Several lessons can be learned from this. First, applying the same surface heat flux pattern that arises from prescribing the 2xCO<sub>2</sub> warming pattern in the slab ocean (SL\_QSfc) returns the same warming pattern, suggesting that, in the absence of CO<sub>2</sub> forcing, there may be a one-to-one correspondence between changes in sea-surface heat fluxes and SSTs. Additionally, the resulting feedbacks in SL\_QSfc are nearly identical to those within SL\_2xCO<sub>2</sub> and SST\_2xCO<sub>2</sub> (Fig. 3a). Comparing SL\_2xCO<sub>2</sub> and SL\_QTOA shows that identical patterns of forcing applied at the TOA or surface, respectively, produce nearly identical temperature responses and feedbacks (Figs. 2b, 3b). The exception to this is near the poles, where the response has been shown to be sensitive to the vertical distribution of forcing [*Payne et al.*, 2015; *Cronin and Jansen*, 2016]. Importantly, all ‘2xCO<sub>2</sub> Variant’ simulations produce similar patterns of surface warming and radiative feedbacks, despite their very different patterns of applied forcing. These findings suggest that, at least in this model configuration, the same pattern of radiative feedbacks will arise whenever a particular pattern of SST change is produced, regardless of whether that pattern was driven by CO<sub>2</sub> forcing, OHU, or simply prescribed. An interpretation of radiative forcing and OHU efficacy, then, is that a given forcing induces a pattern of surface temperature change that, in turn, generates a pattern of radiative feedbacks.

To further highlight the importance of the surface warming pattern for radiative feedbacks, we perform a simulation of prescribed uniform warming of ~3.01 K (denoted SST\_CTL3K); the value 3.01 K is the global mean temperature increase from a doubling of CO<sub>2</sub> (SL\_2xCO<sub>2</sub>; see Fig. 1b). This type of experiment is commonly used as a surrogate for greenhouse gas-induced climate change [e.g. *Cess et al.*, 1990]. Although its global mean feedback parameter is roughly the same as that for polar-amplified warming (SST\_2xCO<sub>2</sub> and SL\_2xCO<sub>2</sub>; see Table S1 in supporting information), SST\_CTL3K has a strikingly different pattern of local feedbacks relative to the other ‘2xCO<sub>2</sub> Variants’ simulations (Fig. 3a). That is, different patterns of surface warming drive distinct patterns of radiative feedbacks.

Finally, we investigate the relative importance of forcing versus SST anomalies in driving local feedback changes in the context of the OHU simulations presented in *Rose et al.* [2014]. To do so, we first prescribe OHU patterns— $Q(\varphi)$  in (2)—that are identical to those in *Rose et al.* [2014]: one with OHU in the high-latitudes centered around 65°N/65°S, and one with OHU in the tropics centered on the equator (Fig. 2a), denoted SL\_QHigh and SL\_QTrop, respectively. The area-weighted global-mean OHU is identical in these two simulations:  $\overline{Q_{High}} = \overline{Q_{Low}} = 2 \text{ W/m}^2$ . These idealized patterns were chosen to mimic the patterns of transient OHU seen in coupled GCM simulations. As shown in *Rugenstein et al.* [2016], the difference in feedback patterns induced by these distinct OHU patterns may be exaggerated within this aquaplanet setup relative to simulations with realistic land geometry; these simulations may thus be viewed as an extreme test of mechanisms governing feedback variations. Similar to *Rugenstein et al.* [2016], we also perform a simulation whereby a uniform uptake of  $2 \text{ W/m}^2$  is applied (denoted SL\_QUni). We refer to this set of three experiments as the ‘Rose-Style’ slab ocean simulations.

Consistent with the results of *Rose et al.* [2014], we see that distinct patterns of OHU drive distinct patterns of temperature response (Fig. 2b), despite the global-mean surface heat flux being identical across simulations. SL\_QHigh and SL\_QTrop both exhibit surface cooling relative to the control, with SL\_QHigh cooling more than SL\_QTrop, especially near the poles. SL\_QUni shows cooling with a magnitude between SL\_QHigh and SL\_QTrop. The radiative feedbacks across these simulations are distinct from each other (Fig. 3b)—as they must be to account for different amounts of cooling under the same global-mean forcing—and are distinct from all ‘2xCO<sub>2</sub> Variant’ simulations. In good agreement with *Rose et al.* [2014] and *Rugenstein et al.* [2016], we find that radiative feedbacks are most positive when OHU is applied at high latitudes, most negative when applied at low latitudes, and in between these extremes when applied uniformly (see Table S1 in the supporting information).

Taken at face value, these results suggest that the pattern of local radiative feedbacks is sensitive to the pattern of surface heat flux changes, consistent with the interpretations provided by *Rose et al.* [2014] and *Winton et al.* [2010]. Yet, different surface temperature patterns are generated by the different surface heat flux patterns—which both *Rose et al.* [2014] and *Winton et al.* [2010] note—meaning that, considering this set of experiments alone, it is ambiguous which mechanism is responsible for the changing feedbacks. This motivates another set of simulations with equivalent prescribed SST patterns, allowing the surface heat fluxes to vary. To compare directly back to the ‘Rose-Style Slab’ runs, we take the equilibrium SST patterns from SL\_QHigh, SL\_QTrop and SL\_QUni and prescribe them in three simulations called SST\_QHigh, SST\_QTrop and SST\_QUni, respectively. These prescribed SST simulations produce feedback patterns that agree well with the OHU-driven slab runs (Fig. 3b): SST\_QHigh gives positive feedbacks in the subtropics, SST\_QTrop gives feedbacks that are more negative at all latitudes than SST\_QHigh, and SST\_QUni gives feedbacks that are roughly between SST\_QTrop and SST\_QHigh. However, there are differences in the subtropical feedbacks that are large enough to require further investigation by future studies. We speculate this may be due to differences in the surface heat fluxes between prescribed SST and prescribed OHU simulations (Fig. S2), however it is still unclear why similarly large differences in sea-surface heat fluxes produced consistent patterns of radiative feedbacks under CO<sub>2</sub> forcing (Figs. 1 and S1).

## 4 Discussion and Conclusions

This study evaluates the validity of prescribed SST simulations for studying radiative feedbacks by independently examining to what extent local radiative feedbacks depend on the pattern of SST change or the nature of the forcing applied. The results shown here imply that nearly the same patterns of radiative feedback arise for a given pattern of SST change, independent of how that SST pattern is induced. Feedbacks thus appear to be largely insensitive to the pattern of TOA radiation or surface heat fluxes that accompany those SST changes. This suggests that studies showing feedbacks to be sensitive to the pattern of forcing [e.g. *Winton et al.* 2010; *Rose et al.* 2014] may equivalently be viewed in terms of feedbacks depending on the resulting patterns of temperature change. In this interpretation, forcing ‘efficacies’ arise from the surface temperature response induced by radiative forcing or OHU—provided that the tropospheric-adjusted forcing framework is used so that the TOA radiative response can be uniquely associated with surface temperature changes. These results show how what could be interpreted as different perspectives in the literature relate to each other: radiative feedbacks fundamentally depend on the pattern of surface temperature change [e.g. *Armour et al.*, 2013; *Andrews et al.* 2015; *Gregory and Andrews* 2016; *Zhou et al.*, 2016], but they also depend on the pattern of forcing applied [e.g. *Winton et al.*, 2010; *Rose et al.*, 2014] through the temperature patterns that forcing induces [e.g. *Shindell et al.*, 2014; *Marvel et al.*, 2015; *Rugenstein et al.*, 2016].

Our interpretation of these findings is that the physical processes governing TOA radiative response primarily depend on temperature changes, rather than on local heat fluxes. The TOA radiative response associated with the Planck feedback illustrates this behavior most simply: it explicitly depends on only local surface temperature change (e.g., *Armour et al.* 2013, *Feldl and Roe* 2013). Lapse-rate, water vapor and cloud distributions have similarly been linked to patterns of sea-surface temperature (e.g., *Shukla and Wallace* 1983; *Lau and Nath* 1994; *Flannaghan et al.* 2014), as have patterns of atmospheric circulation and rainfall (e.g., *Folland et al.* 1986; *Lau and Nath* 1996; *Nobre and Shukla*, 1996; *Chang et al.* 2000). It is thus not surprising that the TOA radiative response is similarly set by the pattern of surface warming. However, it is less clear whether the ice-albedo feedback (absent in our simulations) will behave similarly, given that the relationship between ice concentration and surface temperature is complex when outside of the summer melt season.

There are several caveats to the results presented here. One is that moderately different feedbacks might arise from identical SST patterns if the patterns of surface heat fluxes are sufficiently different, especially in the subtropics (Fig. S2). It also has yet to be seen to what extent our results apply to more realistic simulations, for example with land and sea ice, where temperature changes cannot be prescribed in the same way we have illustrated here. Moreover, feedbacks have also been shown to change by a smaller amount in more realistic simulations [*Rugenstein et al.*, 2016]. These results should thus be verified within more realistic atmospheric GCM simulations that include land, sea ice and a seasonal cycle.

Ancillary to our results, we find that a uniform warming leads to a distinct pattern of radiative feedbacks relative to those under polar amplified warming. This finding is expected given that local feedbacks depend sensitively on the warming pattern. Thus, caution should be exercised in using uniform warming simulations as a surrogate for the response to CO<sub>2</sub> forcing [e.g. *Cess et al.* (1990), CMIP5’s ‘amip4K’ simulations]. However, indeed most importantly, our results do imply that simulations in which the *pattern* of SSTs is prescribed—without the accompanying radiative or OHU forcing that would have given rise to those SSTs—may be useful in studying the feedback response to patterns of temperature



change [e.g., *Gregory and Andrews, 2016; Zhou et al., 2016*]. In particular, this suggests that the upcoming Cloud Feedback Model Intercomparison Project [CFMIP; *Webb et al., 2016*], which will simulate the radiative response to observed SST patterns, will be useful in understanding how radiative feedbacks have changed over the historical period. These results are also particularly encouraging in light of the fact that historical radiative forcing and sea-surface heat flux anomalies are far less well quantified than historical temperature changes.

It is important to note that even though radiative feedbacks appear to be primarily set by the pattern of surface warming, that pattern itself will depend on OHU, TOA forcings and even feedbacks themselves [*Rose et al., 2014; Roe et al., 2015; Rugenstein et al., 2016*]. Thus, coupled model simulations remain critical tools for future climate prediction. Moreover, simulations that include or prescribe surface heat fluxes rather than SSTs [e.g., *Rose et al., 2014; Rugenstein et al., 2016*] remain valuable tools for studying the role of both ocean dynamics and radiative feedbacks on the patterns of the SST response; they additionally have the nice property that they are thermodynamically consistent at the sea surface, making them more suitable to the study of global energy imbalance.

Our findings suggest that a unique pattern of radiative feedbacks will arise from a given pattern of SST change, whether that temperature change is induced by climate forcing or simply prescribed. These results lend support to recent and upcoming studies that prescribe SST changes within large-scale GCMs to examine the response of radiative feedbacks to changing warming patterns [e.g. *Gregory and Andrews, 2016; Zhou et al., 2016; Webb et al., 2016*]. These findings further suggest that what might be seen as different explanations for the inconstancy of radiative feedbacks actually reflect the same mechanisms at work.

## 5 Acknowledgements

All output data, including data used to generate the figures shown in this study, are available upon request from ADH (email: [ahaugsta@uw.edu](mailto:ahaugsta@uw.edu)). We thank the Tamaki Foundation for funding this work. BEJR was supported by NSF grant AGS-1455071.

## 6 References

- Andrews, J. and P.M. Forster (2008), CO<sub>2</sub> forcing induces semi-direct effects with consequences for climate feedback interpretations. *Geophys. Res. Lett.*, 35, L04802, doi:10.1029/2007GL032273
- Andrews, T., J. Gregory, and M. Webb (2015), The Dependence of Radiative Forcing and Feedback on Evolving Patterns of Surface Temperature Change in Climate Models. *J. Climate*, 28, 1630–1648, doi: 10.1175/JCLI-D-14-00545.1.
- Armour, K.C. (2016), Projection and prediction: Climate sensitivity on the rise. *Nature Climate Change*, 6, 896-897, doi:10.1038/nclimate3079.
- Armour, K.C., C.M. Bitz, and G.H. Roe (2013), Time-varying climate sensitivity from regional feedbacks. *Journal of Climate*, 26, 4518–4534, doi: 10.1175/JCLI-D-12-

00544.1.

Armour, K.C., J. Marshall, J. Scott, A. Donohoe and E. R. Newsom (2016), Southern Ocean warming delayed by circumpolar upwelling and equatorward transport. *Nature Geoscience*, 9, 549–554, doi: 10.1038/ngeo2731.

Armour, K. C. (2017) Energy budget constraints on climate sensitivity in light of inconstant climate feedbacks, *Nature Climate Change*, doi: 10.1038/nclimate3278.

Cess, R.D., G.L. Potter, J.P. Blanchet, G.J. Boer, A.D. Del Genio, M. Deque, V. Dymnikov, V. Galin, W.L. Gates, S.J. Ghan, J.T. Kiehl, A.A. Lacis, H. Le Treut, Z.-X. Li, X.-Z. Liang, B.J. McAvaney, V.P. Meleshko, J.F.B. Mitchell, J.-J. Morcrette, D.A. Randall, L. Rikus, E. Roeckner, J.F. Royer, U. Schlese, D.A. Sheinin, A. Slingo, A.P. Sokolov, K.E. Taylor, W.M. Washington, R.T. Wetherald, I. Yagai, and M.-H. Zhang (1990), Intercomparison and interpretation of climate feedback processes in 19 atmospheric general circulation models. *J. Geophys. Res.*, 95, 16601-16615, doi:10.1029/JD095iD10p16601.

Chang, P., Saravanan, R., Ji, L., & Hegerl, G. C. (2000). The effect of local sea surface temperatures on atmospheric circulation over the tropical Atlantic sector. *Journal of Climate*, 13(13), 2195-2216.

Cronin, T. W., and M. F. Jansen (2016), Analytic radiative-advective equilibrium as a model for high-latitude climate. *Geophysical Research Letters*, 43, 449–457, doi:10.1002/2015GL067172

Flato, G., J. Marotzke, B. Abiodun, P. Braconnot, S.C. Chou, W. Collins, P. Cox, F. Driouech, S. Emori, V. Eyring, C. Forest, P. Gleckler, E. Guilyardi, C. Jakob, V. Kattsov, C. Reason and M. Rummukainen, 2013: *Evaluation of Climate Models. In: Climate Change 2013: The Physical Science Basis. Contribution of Working Group I to the Fifth Assessment Report of the Intergovernmental Panel on Climate Change* [Stocker, T.F., D. Qin, G.-K. Plattner, M. Tignor, S.K. Allen, J. Boschung, A. Nauels, Y. Xia, V. Bex and P.M. Midgley (eds.)]. Cambridge University Press, Cambridge, United Kingdom and New York, NY, USA.

Feldl, N. and G. H. Roe (2013) Four perspectives on climate feedbacks, *Geophys. Res. Lett.*, 40, 4007-4011.

Flannaghan, T. J., S. Fueglistaler, I. M. Held, B. Wyman, M. Zhao (2014) Tropical temperature trends in Atmospheric General Circulation Model simulations and the impact of uncertainties in observed SSTs, *J. Geophys. Res. Atmos.*, 19, 13,327–13,337.

Folland, C. K., Palmer, T. N., & Parker, D. E. (1986). Sahel rainfall and worldwide sea temperatures, 1901–85. *Nature*, 320(6063), 602-607.

Forster, P.M. (2016), Inference of Climate Sensitivity from Analysis of Earth's Energy

Budget, *Annual Review of Earth and Planetary Sciences*, 44, 85-106, doi: 10.1146/annurev-earth-060614-105156

Frölicher, T. L., M. Winton, and J. L. Sarmiento (2013), Continued global warming after CO<sub>2</sub> emissions stoppage, *Nature Climate Change*, 4, 40-44, doi:10.1038/nclimate2060.

GFDL Global Atmospheric Model Development Team (2004), The new GFDL global atmosphere and land model AM2–LM2: Evaluation with prescribed SST simulations. *Journal of Climate*, 17, 4641–4673.

Gregory, J. M., and T. Andrews (2016), Variation in climate sensitivity and feedback parameters during the historical period, *Geophys. Res. Lett.*, 43, 3911–3920, doi:10.1002/2016GL068406.

Gregory, J.M., W.J. Ingram, M.A. Palmer, G.S. Jones, P.A. Stott, R.B. Thorpe, J.A. Lowe, T.C. Johns, K.D. Williams (2004), A new method for diagnosing radiative forcing and climate sensitivity. *Geophys. Res. Lett.*, 31, doi: 10.1029/2003GL018747.

Hansen, J., M. Sato, R. Ruedy, L. Nazarenko, A. Lacis, G.A. Schmidt, G. Russell, I. Aleinov, M. Bauer, S. Bauer, N. Bell, B. Cairns, V. Canuto, M. Chandler, Y. Cheng, A. Del Genio, G. Faluvegi, E. Fleming, A. Friend, T. Hall, C. Jackman, M. Kelley, N.Y. Kiang, D. Koch, J. Lean, J. Lerner, K. Lo, S. Menon, R.L. Miller, P. Minnis, T. Novakov, V. Oinas, J.P. Perlwitz, J. Perlwitz, D. Rind, A. Romanou, D. Shindell, P. Stone, S. Sun, N. Tausnev, D. Thresher, B. Wielicki, T. Wong, M. Yao, and S. Zhang (2005), Efficacy of climate forcings. *J. Geophys. Res.*, 110, D18104, doi:10.1029/2005JD005776.

Kang, S.M. and S. Xie, (2014), Dependence of Climate Response on Meridional Structure of External Thermal Forcing. *Journal of Climate*, 27, 5593–5600, doi: 10.1175/JCLI-D-13-00622.1.

Knutti R., M.A.A. Rugenstein (2015), Feedbacks, climate sensitivity and the limits of linear models. *Phil. Trans. R. Soc. A*, 373, <http://dx.doi.org/10.1098/rsta.2015.0146>

Lau, N. C., & Nath, M. J. (1994). A modeling study of the relative roles of tropical and extratropical SST anomalies in the variability of the global atmosphere-ocean system. *Journal of Climate*, 7(8), 1184-1207.

Lau, N. C., & Nath, M. J. (1996). The role of the “atmospheric bridge” in linking tropical Pacific ENSO events to extratropical SST anomalies. *Journal of Climate*, 9(9), 2036-2057.

Marshall J., J. Scott, K. C. Armour, J.-M. Campin, M. Kelley and A. Romanou (2015), The ocean’s role in the transient response of climate to abrupt greenhouse gas forcing. *Climate Dynamics*, 4, 2287–2299, doi: 10.1007/s00382-014-2308-0

Marvel, K., G.A. Schmidt, R.L. Miller, and L. Nazarenko, (2015), Implications for climate sensitivity from the response to individual forcings. *Nature Clim. Change*, 6, no. 4,

386-389, doi:10.1038/nclimate2888.

Murphy, J. (1995), Transient Response of the Hadley Centre Coupled Ocean-Atmosphere Model to Increasing Carbon Dioxide. Part 1: Control Climate and Flux Adjustment. *J. Climate*, 8, 36–56, doi: 10.1175/1520-0442(1995)008<0036:TROTHC>2.0.CO;2.

Nobre, P., & Shukla, J. (1996). Variations of sea surface temperature, wind stress, and rainfall over the tropical Atlantic and South America. *Journal of Climate*, 9(10), 2464-2479.

Payne, A. E., M. F. Jansen and T. W. Cronin (2015), Conceptual model analysis of the influence of temperature feedbacks on polar amplification. *Geophys. Res. Lett.*, 42, doi:10.1002/2015GL065889.

Panyter, D. J., T. L. Frölicher (2015), Sensitivity of radiative forcing, ocean heat uptake and climate feedback to changes in anthropogenic greenhouse gases and aerosols. *J. Geophys. Res. Atmos.* 120, 9837-9854.

Roe, G.H., N. Feldl, K.C. Armour, Y.-T. Hwang and D.M.W. Frierson (2015), The remote impacts of climate feedbacks on regional climate predictability. *Nature Geoscience*, 8, 135-139, doi: 10.1038/ngeo2346.

Rose, B.E.J., K.C. Armour, D.S. Battisti, N. Feldl, D.D.B. Koll (2014), The dependence of transient climate sensitivity and radiative feedbacks on the spatial pattern of ocean heat uptake. *Geophys. Res. Lett.*, 41, doi: 10.1002/2013GL058955.

Rose, B.E.J. and L. Rayborn (2016), The effects of ocean heat uptake on transient climate sensitivity. *Curr. Clim. Change Rep*, 2, 190-201, doi:10.1007/s40641-016-0048-4

Rugenstein, M. A. A., K. Caldeira, and R. Knutti (2016), Dependence of global radiative feedbacks on evolving patterns of surface heat fluxes, *Geophys. Res. Lett.*, 43, 9877–9885, doi:10.1002/2016GL070907.

Rugenstein, M. A. A., J. M. Gregory, N. Schaller, J. Sedlacek, and R. Knutti (2016b), Multiannual Ocean–Atmosphere Adjustments to Radiative Forcing. *J. Climate*, 29, 5643-5649.

Shukla, J., and Wallace, J. M. (1983). Numerical simulation of the atmospheric response to equatorial Pacific sea surface temperature anomalies. *Journal of the Atmospheric Sciences*, 40(7), 1613-1630.

Lau, N. C., and Nath, M. J. (1994). A modeling study of the relative roles of tropical and extratropical SST anomalies in the variability of the global atmosphere-ocean system. *Journal of Climate*, 7(8), 1184-1207.

Tan, Z., T. Schneider, J. Teixeira, and K. G. Pressel (2017), Large-eddy simulation of subtropical cloud-topped boundary layers: 2. Cloud response to climate change, *J. Adv. Model. Earth Syst.*, 9, doi:10.1002/2016MS000804.

Trossman, D. S., J. B. Palter, T. M. Merlis, Y. Huang, and Y. Xia (2016), Large-scale ocean circulation-cloud interactions reduce the pace of transient climate change, *Geophys. Res. Lett.*, 43, 3935–3943, doi:10.1002/2016GL067931.

Senior, C.A. and J.F.B Mitchell (2000), The time-dependence of climate sensitivity. *Geophys. Res. Lett.*, 27, 2685-2688.

Shindell, D.T. (2014), Inhomogeneous forcing and transient climate sensitivity. *Nature Clim. Change*, 4, 274-277, doi:10.1038/nclimate2136.

Webb, M., T. Andrews, A. Bodas-Salcedo, et al. (2017) The Cloud Feedback Model Intercomparison Project (CFMIP) contribution to CMIP6. *Geosci. Model Dev.*, 10, 359–384.

Williams, K., W. Ingram, and J. Gregory (2008), Time Variation of Effective Climate Sensitivity in GCMs. *J. Climate*, 21, 5076–5090, doi: 10.1175/2008JCLI2371.1.

Winton, M., K. Takahashi, and I. Held (2010), Importance of Ocean Heat Uptake Efficacy to Transient Climate Change. *J. Climate*, 23, 2333–2344, doi: 10.1175/2009JCLI3139.1.

Zhou, C., M.D. Zelinka, S.A. Klein (2016), Impact of decadal cloud variations on the Earth's energy budget. *Nature Geoscience*, doi: 10.1038/NGEO2828.

Accepted Article

**Table 1.** All simulations follow the same general setup as described in section 2 unless otherwise indicated. SL\_2xCO2 is the only slab ocean run that does not have a prescribed ocean heat uptake **(a)** Outlines the slab (SL\_) simulations **(b)** Outlines the prescribed sea-surface temperature (SST\_) simulations, with SST profiles taken from corresponding slab runs.

**(a)**

Simulation (full name)	Abbreviation	Description
Slab Ocean Control	SL_CTL	Control run in slab ocean configuration. Control greenhouse gas concentrations are 348 ppmv CO <sub>2</sub> , 1650 ppbv CH <sub>4</sub> , and 306 ppbv N <sub>2</sub> O. All subsequent simulations are run with these concentrations unless otherwise indicated
Doubled CO <sub>2</sub>	SL_2xCO <sub>2</sub>	CO <sub>2</sub> value doubled from 348 ppm to 696 ppm
High Latitude Uptake	SL_QHigh	High latitude uptake profile (Q <sub>High</sub> ) from <i>Rose et al.</i> [2014] applied as surface heat flux
Tropical Uptake	SL_QTrop	Tropical latitude uptake (Q <sub>low</sub> ) profile from <i>Rose et al.</i> [2014] applied as surface heat flux
Uniform Uptake	SL_QUni	2 W/m <sup>2</sup> uptake applied uniformly at all grid points
Doubled CO <sub>2</sub> TOA Change Applied as Surface Heat Flux	SL_QTOA	TOA radiative forcing profile associated with a doubling of CO <sub>2</sub> applied as surface heat flux
Doubled CO <sub>2</sub> SFC Flux Change Applied as Surface Heat Flux	SL_QSfc	Surface radiative flux changes from SST_2xCO <sub>2</sub> simulation re-applied as surface heat flux

**(b)**

Simulation (full name)	Abbreviation	Description
Prescribed SST Control	SST_CTL	Control run in prescribed SST configuration. Prescribed SST pattern taken from SL_CTL simulation
Doubled CO <sub>2</sub> Prescribed SST	SST_2xCO <sub>2</sub>	Prescribed SST pattern taken from SL_2xCO <sub>2</sub> simulation
Control Prescribed SST with a Doubling of CO <sub>2</sub>	SST_CTLw/2xCO <sub>2</sub>	Prescribed SST taken from CTL, with CO <sub>2</sub> doubled (696 ppm)
Control Prescribed SST plus ~3K	SST_CTL3K	Prescribed SST taken from CTL, with temperatures increased by 3.01K
Doubled CO <sub>2</sub> Prescribed SST with a Doubling of CO <sub>2</sub>	SST_2xCO <sub>2</sub> w/2xCO <sub>2</sub>	Prescribed SST taken from 2xCO <sub>2</sub> , with CO <sub>2</sub> doubled (696 ppm)
High Latitude Uptake Prescribed SST	SST_QHigh	Prescribed SST taken from SL_QHigh simulation
Tropical Latitude Uptake Prescribed SST	SST_QTrop	Prescribed SST taken from SL_QTrop simulation
Uniform Uptake Prescribed SST	SST_QUni	Prescribed SST taken from SL_QUni run

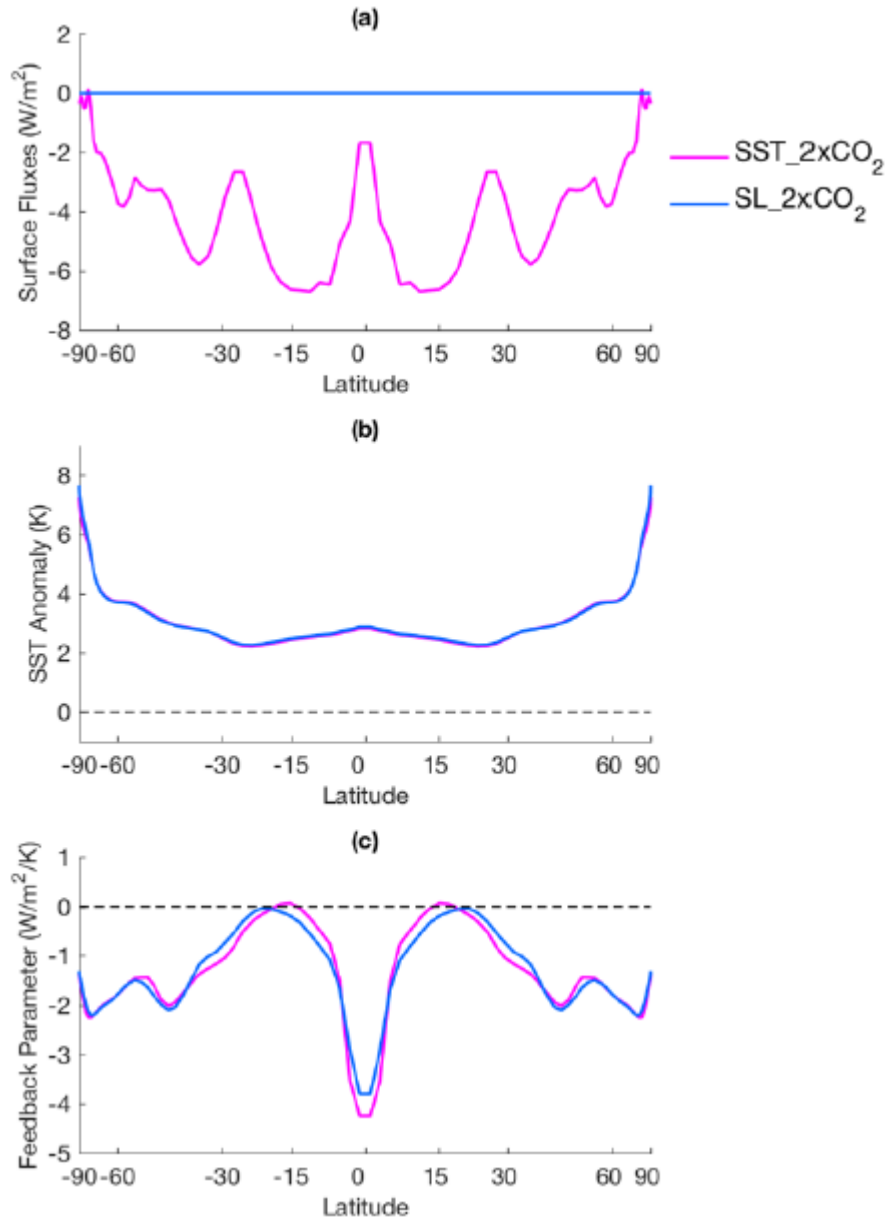


**Figure 1.** Zonal-mean (a) surface heat flux changes, (b) sea-surface temperature (SST) changes, and (c) radiative feedbacks resulting from a doubling of atmospheric CO<sub>2</sub> within the slab ocean (SL\_2xCO<sub>2</sub>) and from a simulation with the same pattern of SST change prescribed (SST\_2xCO<sub>2</sub>), allowing the system to equilibrate in each case. Variables are shown weighted by sine of latitude to weight by surface area and are symmetrized about the equator. For surface fluxes, negative values correspond to heat being released by the ocean (negative ocean heat uptake).

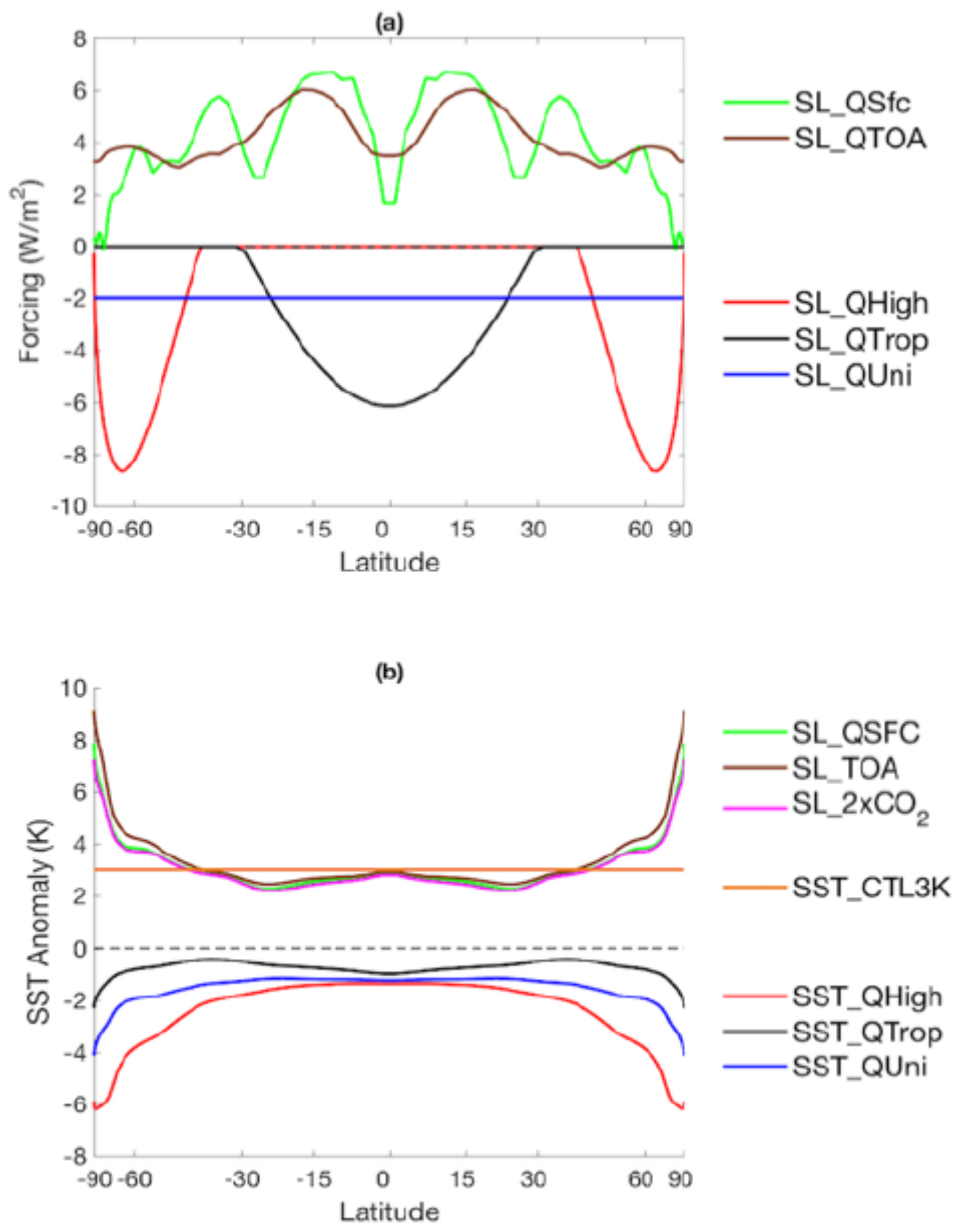


**Figure 2.** Zonal-mean (a) surface heat flux or TOA radiation changes and (b) sea-surface temperature (SST) changes, for the simulations summarized in Table 1, again allowing the system to equilibrate in each case. Variables are shown weighted by sine of latitude to weight by surface area, and are symmetrized about the equator. For forcings, negative values correspond to heat being taken up by the ocean (positive ocean heat uptake), whereas positive values correspond to heat being released by the ocean (negative ocean heat uptake).



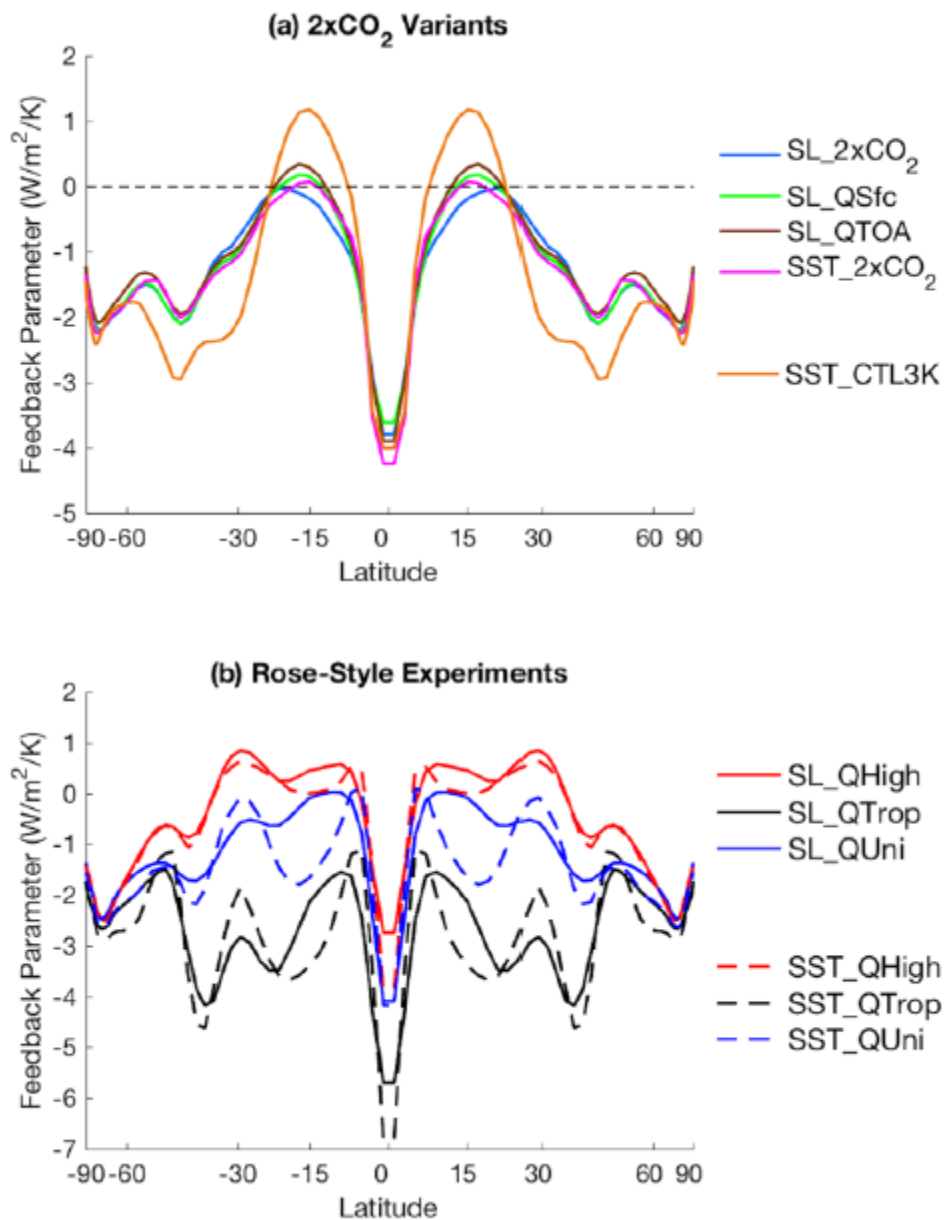


**Figure 3.** Equilibrium zonal mean radiative feedbacks arising from (a) ‘2xCO<sub>2</sub> variant’ simulations and (b) ‘Rose-Style’ simulations (summarized in Table 1). Variables are shown weighted by sine of latitude to weight by surface area, and are symmetrized about the equator.